Journal of
Mechanical
Science and
Technology

Journal of Mechanical Science and Technology 21 (2007) 1018~1027

Control of Two-Axis Pneumatic Artificial Muscle Manipulator with a New Phase Plane Switching Control Method

TU Diep Cong Thanh[b], Kyoung Kwan AHN[a,*]

[a] *School of Mechanical and Automotive Engineering, University of Ulsan, Korea*
[b] *Mechatronics Department, Ho Chi Minh City University of Technology, Viet Nam*

(Manuscript Received September 25, 2006; Revised April 24, 2007; Accepted April 24 2007)

Abstract

The use of robots in rehabilitation has become an issue of increasing importance because of the requirement of functional recovery therapy for limbs. A novel pneumatic artificial muscle (PAM) actuator – which has achieved increased popularity for providing safety and mobility assistance to humans performing tasks, as well as providing another advantages such as high strength and power/weight ratio, low cost, compactness, ease of maintenance, cleanliness, readily available, cheap power source, and so on – has been considered during the recent decades for use in a therapy robot, which in particular requires a high level of safety. However, some limitations still exist, such as air compressibility and the lack of damping ability of the actuator to bring the dynamic delay of the pressure response and cause the oscillatory motion. In addition, to aid rehabilitation more efficiently, the robot should adjust its impedance parameters according to the physical condition of the patient. For this purpose, the manipulator join is equipped with a Magneto-Rheological Brake (MRB). A new phase plane switching control method using MRB is proposed for tracking sinusoidal waveforms. The effectiveness of the proposed algorithm is demonstrated through an experiment using a fabricated two-axis PAM manipulator. The experiment proves that the stability of the manipulator could be greatly improved using a high gain control without regard to the change of the frequencies of the reference input and the external load condition, and without decreasing the response speed or lowering the stiffness of PAM manipulator.

Keywords: Pneumatic artificial muscle; Phase plane switching control; Manipulator; Magneto-rheological brake

1. Introduction

The number of people requiring rehabilitation due to bone fracture or joint disease caused by traffic accidents and cerebral apoplexy, and for functional motor problems due to advanced age, numbers several hundreds of thousands worldwide. The application of robotics to rehabilitation is thus of great concern. Functional recovery therapy is normally carried out by medical therapists on a person-to-person basis, but automatic equipment has been put to practical use in physical therapy programs that repeat relatively simple operations, such as a continuous passive motion machine, a walking training device, and a torque machine used for a single axis (Doi, 1993; Fujie et al., 1994; Fujie et al., 1995). This research deals with functional recovery therapy, one important aspect of physical rehabilitation. Single-joint therapy machines have already been created (Ahn and Thanh, 2004; 2005a; 2005b). However, multi-joint robots are necessary to achieve more realistic motion patterns, and hence are necessary for more efficient therapy. This kind of robot must have a high level of safety for human use. The PAM manipulator has been used to construct a therapy robot with two degrees of freedom (DOF). A 2-DOF robot for functional recovery therapy driven by pneumatic

*Corresponding author. Tel.: +82 52 259 2282, Fax.: +82 52 259 1680
E-mail address: kkahn@ulsan.ac.kr

muscle was developed by Zobel (Zobel et al., 1999) and Raparelli (Raparelli et al., 2001; 2003) artificial muscle actuators for biorobotic systems by Klute (Klute et al., 1999; 2000; 2002; 2003) a pneumatic muscle hand therapy device by Koeneman (Koeneman et al., 2004) and a human-friendly therapy robot (Thanh and Ahn, 2006a). However, some limitations still exist, such as the air compressibility and the lack of damping ability of the actuator to bring the dynamic delay of the pressure response, causing oscillatory motion. In addition, to execute rehabilitation more efficiently, the robot must adjust its impedance parameters according to the physical condition of the patient. For this purpose, a new technology, an electro-rheological fluid damper (ER Damper), has been applied to the PAM manipulator. Noritsugu and his team used an ER damper to improve the control performance of the PAM manipulator with a PI controller and pulse code-modulated on-off valves (Noritsugu et al., 1994). By separating the region where the damper produces a damping torque to reconcile both damping and response speed under high gain control, the results show that the ER damper is an effective method for use in a practically available, human-friendly robot using the PAM manipulator. Moreover, position control is improved without a decrease in response speed. However, some limitations hamper the technology, since ER Fluid (ERF) requires extremely high control voltage (kV), which is problematic, and in particular, potentially dangerous, only operates in a narrow temperature range (and one unsuitable for PAM manipulators), and exhibits nonlinear characteristics. Because ERF has many unacceptable disadvantages, magneto-rheological fluid (MRF) has been considered an attractive alternative for the advantages listed in Table 1, and has been recently used in human-friendly therapy robots (Thanh and Ahn, 2006b). Though these systems were successful in addressing smooth actuator motion response to step inputs, assuming that two axes PAM manipulator is utilized in therapy robot in the future, which is the final goal of our research, it is necessary to realize fast response, even if the external inertia load changes severely with sinusoidal response without regard to the various frequencies.

Therefore, to realize satisfactory control performance, a MRB is equipped to the joint of the manipulator. A phase plane switching control method using a MRB is proposed for the case of tracking sinusoidal waveforms, and the effectiveness of the proposed algorithm will be demonstrated through the experiments involving a two-axis PAM manipulator. The experiments show that the stability of the manipulator could be greatly improved under a high gain control without regard to variations of the frequencies reference and external load conditions, and without decreasing the response speed and low stiffness of the two-axis PAM manipulator.

2. Experimental setup

2.1 Experimental apparatus

The schematic diagram of the two-axis pneumatic artificial muscle manipulator is shown in Fig. 1. The

Table 1. Comparison of rheological fluids.

	Magneto-Rheological Fluid	Electro-Rheological Fluid
Max. Yield Stress	50 –100 kPa	2 – 5 kPa
Viscosity	0.1 – 1.0 Pa-s	0.1 – 1.0 Pa-s
Operable Temp. Range	-40 to + 150 °C	+10 to + 90 °C (ionic, DC) -25 to + 125 °C (non-ionic, AC)
Stability	Unaffected by most impurities	Cannot tolerate impurities
Response Time	< milliseconds	< milliseconds
Density	3 – 4 g/cm^3	1 – 2 g/cm^3
Max. Energy Density	0.1 Joule/cm^3	0.001 Joule/cm^3
Power Supply	2 – 25 V @ 1 – 2 A (2 – 50 watts)	2 – 25 KV @ 1 – 10 mA (2 – 50 watts)

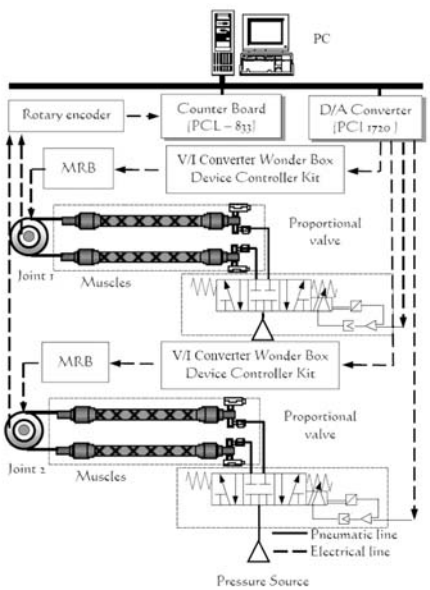

Fig. 1. Schematic diagram of two axes pneumatic artificial muscle manipulator.

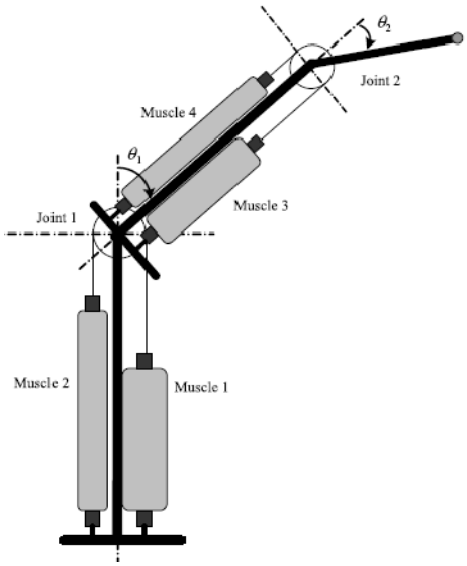

Fig. 2. Working principle of the pneumatic artificial muscle manipulator.

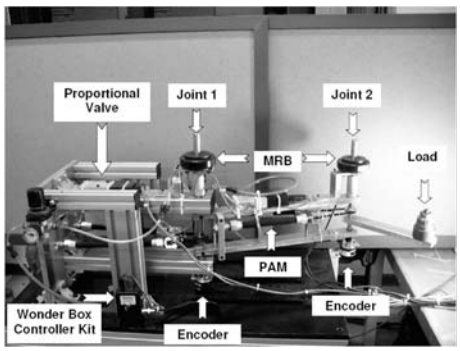

Fig. 3. Photograph of the experimental apparatus.

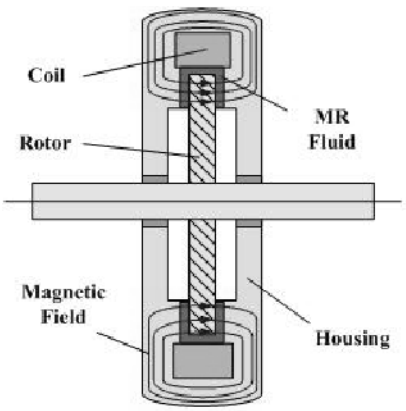

Fig. 4. Construction of MRB.

the pressure difference between the antagonistic artificial muscles and the external load is rotated as a result in Fig. 2. The joint angles, θ_1 and θ_2, were measured with a rotary encoder (METRONIX, S48-8-3600ZO) and fed back to the computer through a 24-bit digital counter board (Advantech, PCL 833). The external inertia load could be varied from 20 [kgf·cm^2] to 40 [kgf·cm^2], a 200 [%] change with respect to the minimum inertia load condition; various frequencies of reference input (sinusoidal) waveform are considered. The experiments are

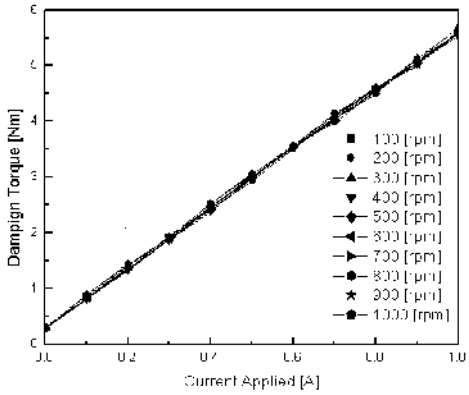

(a)

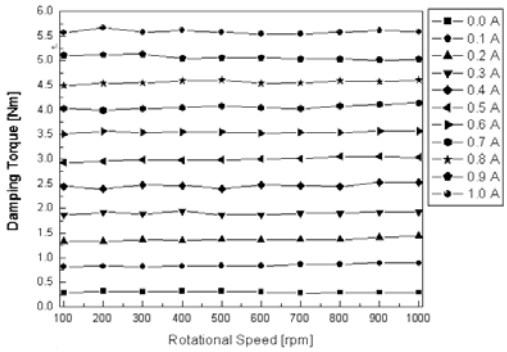

(b)

Fig. 5. Characteristics of MRB.

Table 2. Experimental hardware.

No.	Name	Model name	Company
1	Proportional valve	MPYE-5-1/8HF-710 B	Festo
2	Magneto-Rheological Rotary Brake	MRB-2107-3 Rotary Brake	Lord
3	Pneumatic artificial muscle	MAS-10-N-220-AA-MCFK	Festo
4	D/A board	PCI 1720	Advantech
5	Wonder Box Device Controller Kit	RD-3002-03	Lord
6	Rotary encoder	H40-8-3600ZO	Metronix
7	24-bit digital counter board	PCL 833	Advantech

conducted under an ambient pressure of 0.4 [MPa] and all control software is coded in C program language. A photograph of the experimental apparatus is shown in Fig. 3.

2.2 Characteristics of MRB

The design of the MRB is shown in Fig. 4. The rotor is fixed to the shaft, which can rotate relative to the housing. The gap between the rotor and housing is filled with MRF. The braking torque of the MRB can be controlled by the electric current in its coil. The apparent viscosity of the MRF is changed within a few milliseconds of the application of a magnetic field, and returns to its normal viscosity in the absence of a magnetic field.

The following experiments are performed to investigate the characteristics of MRB; measurement data is reported in Fig. 5 and Table 3. The MRB is connected with a torque transducer and a servomotor in series. In the experiments, the rotational speed is varied from 100 [rpm] to 1000 [rpm] and the applied current from 0 [A] to 1 [A]. These ranges are used because the response of the system does not reach 1000 [rpm] and the maximum current applied for MRB is 1 [A]. Figure 5 shows the damping torque with respect to the change of the input current (a) and rotational speed (b) of MR Brake. From Fig. 5, it is clear that the damping torque of MRB is independent of rotational speed and almost proportional to input current. Thus, Eq. (1) for inputs current I and damping torque T_b

Table 3. Measurement data of MRB.

W / I	0	0.1	0.2	0.3	0.4	0.5	0.6	0.7	0.8	0.9	1
100	0.28	0.81	1.33	1.87	2.44	2.93	3.51	4.03	4.5	5.11	5.57
200	0.31	0.82	1.33	1.92	2.4	2.96	3.57	3.99	4.54	5.12	5.67
300	0.3	0.81	1.36	1.89	2.48	2.99	3.54	4.03	4.55	5.13	5.58
400	0.31	0.82	1.35	1.94	2.46	2.98	3.55	4.05	4.59	5.05	5.62
500	0.31	0.83	1.37	1.87	2.4	2.99	3.55	4.08	4.61	5.06	5.58
600	0.3	0.83	1.36	1.87	2.48	3	3.53	4.05	4.54	5.06	5.55
700	0.28	0.86	1.37	1.9	2.46	3.01	3.54	4.03	4.55	5.04	5.55
800	0.29	0.86	1.37	1.9	2.44	3.05	3.54	4.08	4.59	5.04	5.58
900	0.29	0.89	1.41	1.92	2.53	3.05	3.57	4.11	4.58	5.01	5.61
1000	0.29	0.89	1.44	1.93	2.53	3.04	3.57	4.14	4.61	5.03	5.59

W: Rotational Speed [rpm]
I: Current Applied [A]

$$T_b = f(I) = a + bI \tag{1}$$

Here, a and b are constants determined using characteristic MRB response curve.

3. Control system

3.1 Position control system

To control this PAM manipulator, a conventional PID control algorithm is used as the basic controller in this research. The controller output can be expressed in the time domain as follows:

$$u(t) = K_p e(t) + \frac{K_p}{T_i}\int_0^t e(t)dt + K_p T_d \frac{de(t)}{dt} \tag{2}$$

Taking the Laplace transform of (2) yields

$$U(s) = K_p E(s) + \frac{K_p}{T_i s}E(s) + K_p T_d s E(s) \tag{3}$$

The resulting transfer function of the PID controller is:

$$\frac{U(s)}{E(s)} = K_p\left(1 + \frac{1}{T_i s} + T_d s\right) \tag{4}$$

A typical real-time implementation at sampling sequence k can be expressed as follows:

$$u(k) = K_p e(k) + u(k-1) + \frac{K_p T}{T_i}e(k) + K_p T_d \frac{e(k) - e(k-1)}{T} \tag{5}$$

where $u(k)$ and $e(k)$ are the control input to the control valve and the error between the desired set point and the output of joint, respectively.

In addition, using an MRB is an effective way to improve the control performance of the PAM manipulator by reconciling both the damping and response speed (because it works in only the regions where the acceleration or deceleration is too high). Here, s is Laplace variable, T_a is the torque produced by the manipulator, T_c is constant torque, K_{ED} determines the gain for the torque proportional to the angular speed $\dot{\theta}$, and V_c is a control voltage of source calculated from Eq. (1) to produce T_c. The

direction of the damping torque is opposite to the direction of rotation of the arm. Therefore, Eq. (6) below indicates that the damper produces a damping torque T_b.

$$T_b = \left(K_{ED}\dot{\theta} + T_c\right) sign(\dot{\theta}) \tag{6}$$

The structure of the proposed phase plane switching control method is shown in Fig. 6.

3.2 Conventional phase plane switching control method

Figure 7 shows the conventional phase plane switching control method. In the region in which the joint angle of the arm approaches to the desired angle, *a~b*, *c~d*, in Fig. 7(a), the current is not applied, whereas in the region (the diagonally shaded areas) *b~c*, *d~e,* the current is applied to improve the damping performance for faster convergence to the desired angle. Though the system successfully responds smoothly to step inputs, its quality degrades (and response lengthens) due to sinusoidal waveform reference input of uncontrollable points (c, e and so on). In addition, assuming that two-axis PAM manipulators are utilized in future therapy robots (the final goal of our research), it is necessary to realize a fast response, even if the external inertia load changes severely with sinusoidal response, and one that is independent of frequency over the occurring frequency range.

3.3 Proposition of new concept of phase plane switching control algorithm

The damping torque T_b, which is shown in Eq. 1, improves the damping performance of the manipulator. Since the damping torque acts in the direction opposite the rotational motion of the manipulator, its acceleration performance is degraded. In the region where the joint angle of the arm approaches to the desired angle, $o \sim a, b \sim c, d \sim e, f \sim g$, in Fig. 8(a), the current is not applied since a high response speed is required. In the region where the arm passes through the desired angle, i.e. the diagonally shaded areas of $a \sim b, c \sim d, e \sim f, g \sim h$ in Fig. 8(a), a current is applied to improve the damping performance, so that the arm converges to the desired angle more quickly. To determine whether the magnetic field should be applied, the phase plane

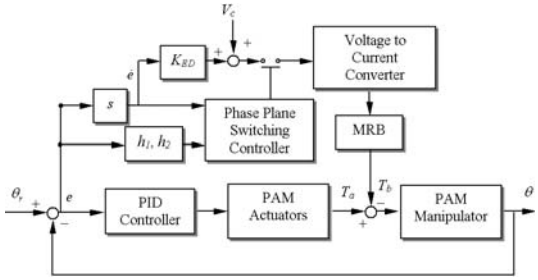

Fig. 6. Block diagram of new concept of phase plane switching control.

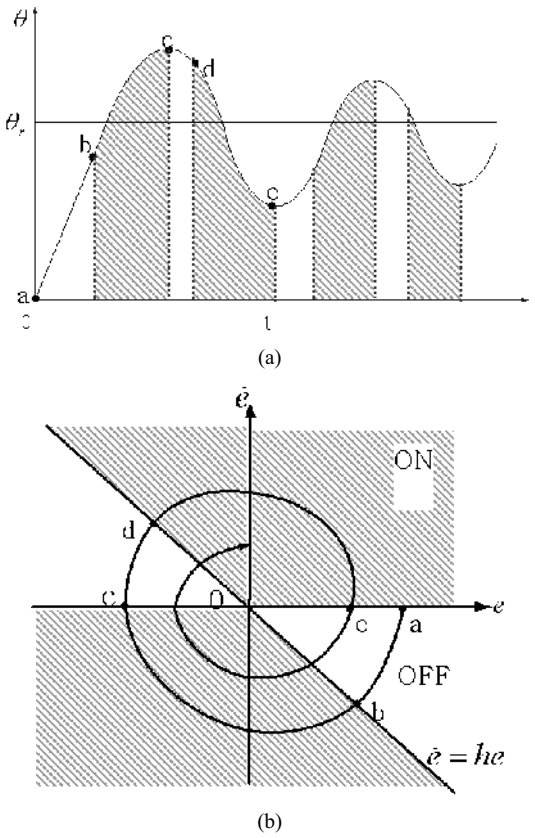

Fig. 7. A conventional phase plane switching control method.

shown in Fig. 8(b) is used.

The horizontal axis in the phase plane corresponds to joint angle deviation e between the desired angle θ_r and the joint angle θ, and the vertical axis corresponds to the time derivative of the deviation, $\dot{e} = \frac{de}{dt} = -\dot{\theta}$. Each point $a \sim h$ on the phase plane corresponds to the likewise lettered point in Fig. 8(a). Here, the region with the application of current are controlled by h_1 (s^{-1}), h_2 (s^{-1}), the gradient of the

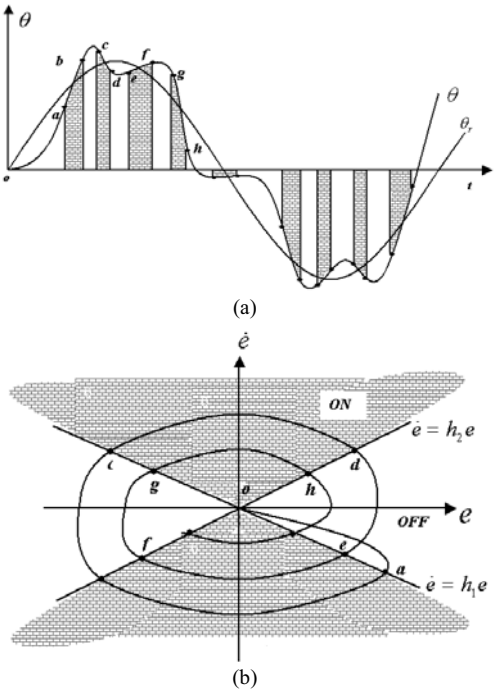

Fig. 8. A new concept of phase plane switching control method.

line shown in Fig. 8(b). The region under the application of the damping torque is controlled as h_1 and h_2. The advantage of controlling the region in which MRB is applied is needed to without decreasing response speed. The effectiveness of proposed controller will be experimentally investigated.

4. Experimental results

In this study, a controller for a two-axis PAM manipulator using the new concept of a phase plane switching controller is fabricated, and experiments are carried out using a sinusoidal waveform as a reference input at two different frequencies (*f=0.3 Hz and 0.5 Hz*). Two external inertial load conditions (*Load 1* = 20 [kgf·cm^2]; *Load 2* = 40 [kgf·cm^2]) are also tested (the loads are attached to the end of Arm 2). In addition, the conventional PID controller and the proposed controller are compared.

Firstly, the experiments are carried out to verify the effectiveness of the proposed controller at various reference input frequencies (of Joint 1). Figure 9 shows the comparison between the conventional PID controller and the proposed controller of experimental result of Joint 1 and the effectiveness of proposed controlled is shown in detail in Fig. 10 with respect to

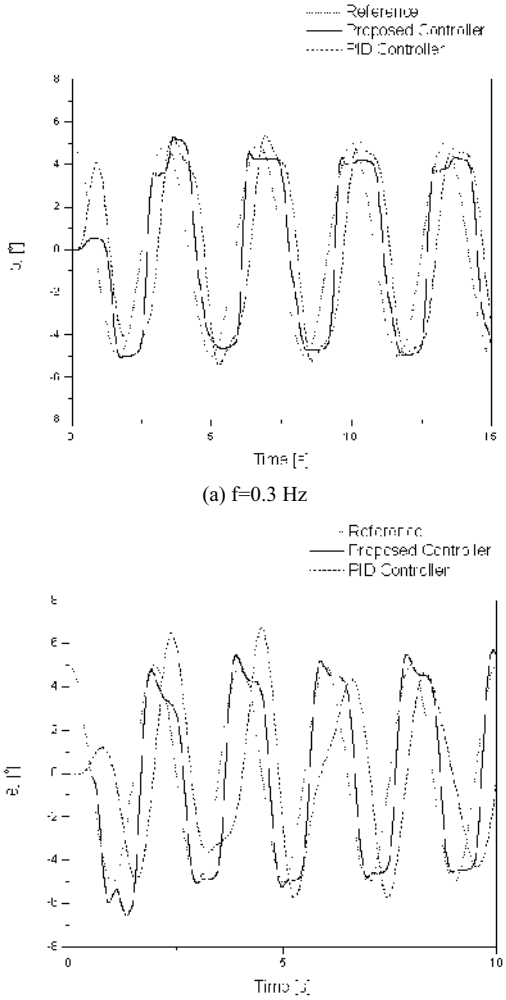

Fig. 9. Comparison between conventional PID controller and proposed controller (*Joint 1*).

f=0.3Hz and f=0.5Hz. In the experiment, the initial values of the proposed controller are set to $K_p = 190\times10^{-6}$, $K_i = 10\times10^{-6}$, $K_d = 150\times10^{-6}$, $K_{ED} = 0.015$, $T_c = 0.8, h_1 = -1, h_2 = 2$. These parameters were obtained by trial-and-error. These experimental results show that there is a large tracking error and time delay with respect to the increase of the frequency of the reference input; when using PID controller the response becomes worse with frequency up to *0.5Hz*, whereas the settling time decreases and the tracking performance is guaranteed by using the proposed controller. The damping torque is not applied for fast response when the manipulator starts to move, and the damping torque is applied by the MRB to the rotational axis of the PAM mani-

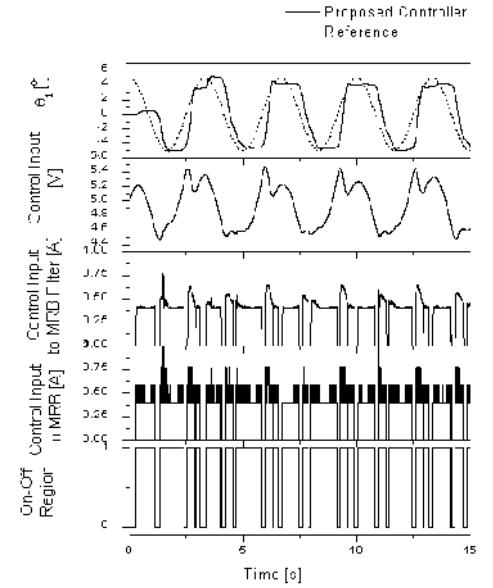

(a) f=0.3 Hz

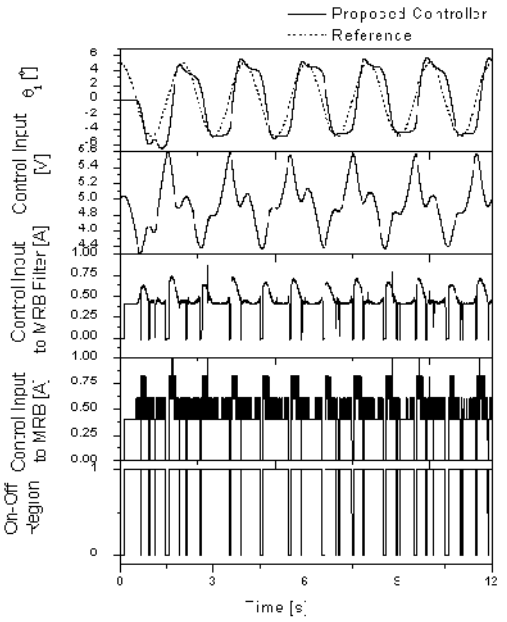

(b) f=0.5 Hz

Fig. 10. Experimental results of the proposed controller (*Joint 1*).

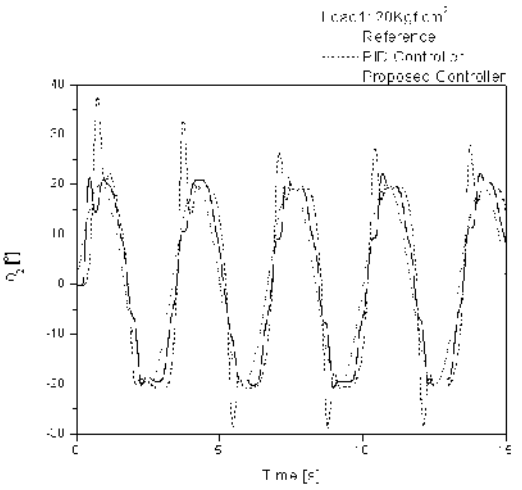

(a) f=0.3 Hz

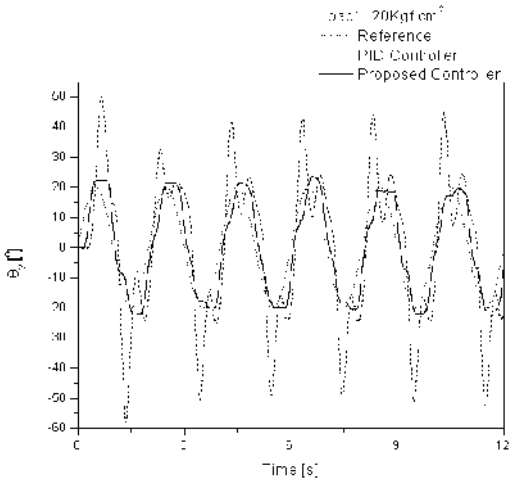

(b) f=0.5 Hz

Fig. 11. Comparison between conventional PID controller and proposed controller (*Joint 2, load 1*).

pulator to reduce the overshoot and oscillation when the manipulator reaches the desired angle.

Next, experiments were carried out to investigate the control performance with respect to the various reference input frequencies (of Joint 2). In addition, the external inertial loads (*Load 1* = 20 [kgf·cm^2]; *Load 2* = 40 [kgf·cm^2]) are attached to the end of arm 2, and the control parameters are set to be the same as Joint 1. Figures 11 and 12 show the comparison between the PID controller and the proposed controller for tested reference input frequencies and external initial load conditions. These figures show that there is a large error and time delay and that more oscillation occurs with respect to increasing reference input frequency, as well as to increasing external initial loads. In the experiments, the PAM manipulator joint angle agrees well with the reference when using the new phase plane switching controller. The effectiveness of the newly proposed phase plane switching control algorithm is also shown in detail in Figs. 13 and 14. The experimental results show that a good control performance and strong robu-stness are

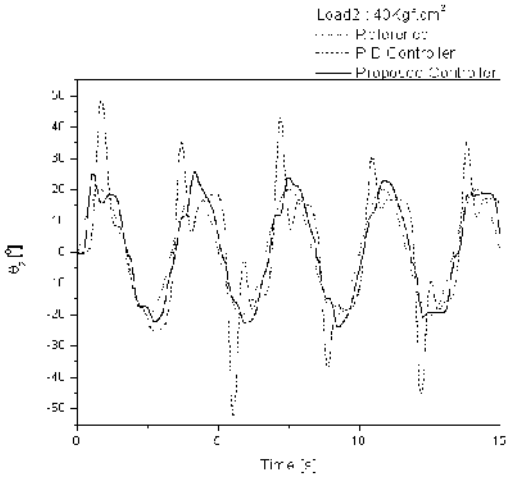

(a) f=0.3 Hz

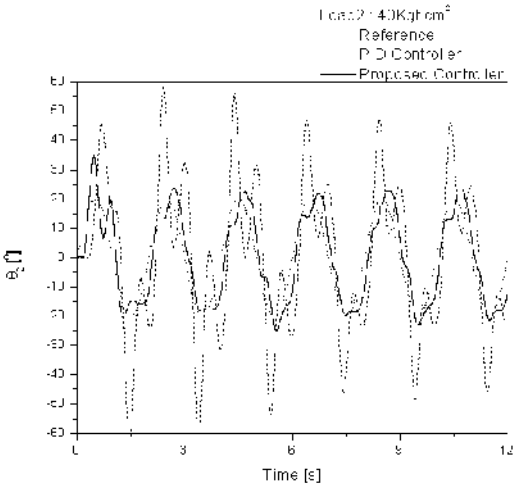

(b) f=0.5 Hz

Fig. 12. Comparison between conventional PID controller and proposed controller (*Joint 2, load 2*).

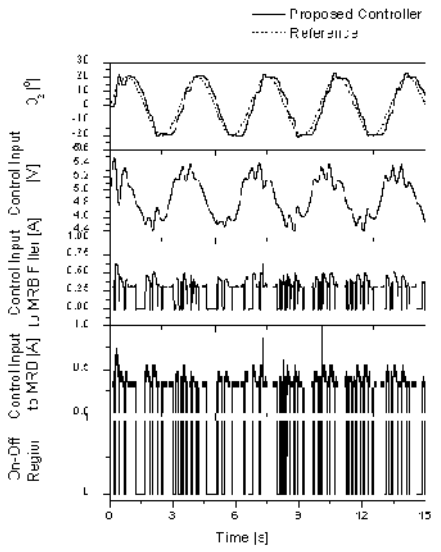

(a) f=0.3 Hz

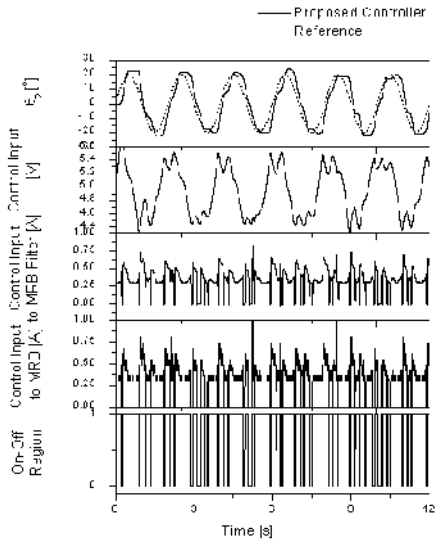

(b) f=0.5 Hz

Fig. 13. Experimental results of the proposed controller (*Joint 2, load 1*).

obtained and do not depend on external initial load when using the proposed control method. These experimental results show that the damping torque is applied and released very frequently according to the approach to the desired angle. It is demonstrated that the proposed algorithm is effective in the case of various external loads and does not depend on reference input frequency. In addition, it is understood that the rotational angle of the PAM manipulator smoothly converges to the desired angle with little oscillation. It is concluded that the newly proposed phase plane switching control algorithm effectively tracks control of a sinusoidal waveform with high gain control, and has good control performance, a fast response, and strong robust stability under varying external inertial loads and reference input frequency.

5. Conclusions

In this study, a new concept of phase plane switching control using a magneto-rheological brake is proposed and applied to a two-axis pneumatic artificial muscle manipulator to improve the control performance under various external loads and independently of reference input frequency.

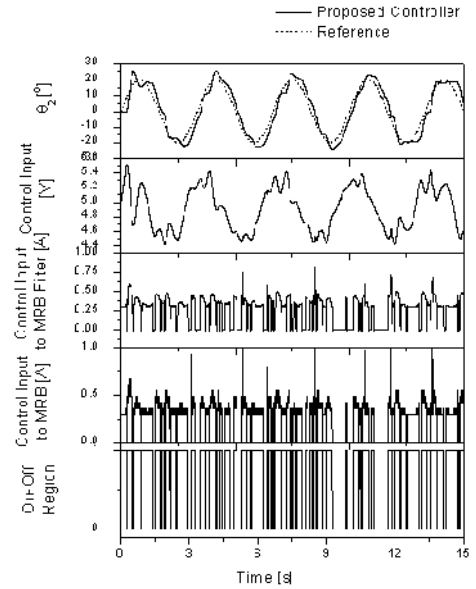

(a) f=0.3 Hz

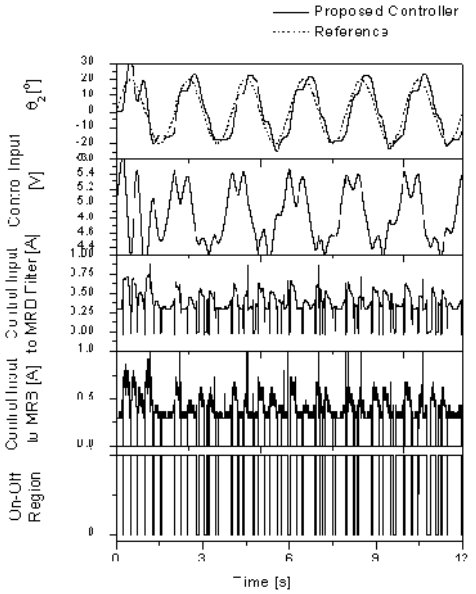

(b) f=0.5 Hz

Fig. 14. Experimental results of the proposed controller (*Joint 2, load 2*).

The experiments showed that the proposed control algorithm was highly effective in the tracking control of a sinusoidal trajectory and had high gain control, good control performance, fast response and strong, robust stability with respect to variation of both external loads and reference input frequency. The results also suggest that the proposed phase plane switching control using MRB is one of the most effective methods for developing a practically available, human-friendly robot by using a PAM manipulator.

Acknowledgement

This work was supported by University of Ulsan, Korea.

References

Ahn, K. K. and Thanh, T. D. C., 2004, "Improvement of the Control Performance of Pneumatic Artificial Muscle Manipulators Using an Intelligent Switching Control Method," *in KSME, Int., Jour.*, Vol. 8, No. 8, pp. 1388~1400.

Ahn, K. K. and Thanh, T. D. C., 2005a, "NOnliear PID Control to Improve the Control Performance of PAM Manipulators Using Neural Network," *in KSME, Int., Jour.*, Vol. 19, No. 1, pp. 106~115.

Ahn, K. K., Thanh, T. D. C. and Ahn, Y. K., 2005b, "Performance Improvement of PAM Manipulators Using Magneto-rheological Brake," *in KSME, Int., Jour.*, Vol. 19, No. 3, pp. 777~790.

Doi, Y., 1993, "Exercise Apparatus for Restoration of Function," *J. Soc. Biomech.*, Vol. 17, No. 2, pp. 99 ~105.

Fujie, M. G., Tani T., Hirano, K., Yoshida, T. and Wada, N., 1994, "Walking Rehabilitation System for the El-derly," *in Proc., IEEE Int., Conf., Advanced Robotic Systems*, Vol. 3, pp. 1655~1662.

Fujie, M. G., Tani T., Hirano, K., Yoshida, T. and Wada, N., 1995, "Improvement of Walking Rehabilitation System for Elderly," *in Proc. IEEE Int. Conf. Robotics and Automation*, Vol. 3, pp. 32~39.

Klute, G. K., Czerniecki, J. and Hannaford, B., 1999, "McKibben Artificial Muscles: Actuators with Biomechanical Intelligence," *Proc., IEEE/ASME Int., Conf., Advanced Intelligent Mechatronics*, pp. 221~226.

Klute, G. K., Czerniecki, J. and Hannaford, B., 2000, "Artificial Tendons: Biomechanical Properties for Prosthetic Lower Limbs," *in Proc., IEEE Int., Conf., Medical Physics and Biomedical Engineering*, Vol. 3, pp. 1972~1975.

Klute, G. K., Czerniecki, J. and Hannaford, B., 2003, "Muscle-Like Pneumatic Actuators for Below-Knee Prostheses," *Proc. Int., Conf., New Actuators*, pp. 289~292.

Klute, G. K., Czerniecki, J. M. and Hannaford, B., 2002 "Artificial Muscles: Actuators for Biorobotic Systems," Accepted for Publication, *Int., Jour., Robotics*

Research

Koeneman, E. J., Schultz, R. S., Wolf, S. L., Herring, D. E. and Koeneman, J. B., 2004, "A Pneumatic Muscle Hand Therapy Device," *in Proc., IEEE/EMBS Int., Conf.*, pp. 2711~2713.

Noritsugu, T, Tsuji, Y. and Ito, K., 1994, "Improvement of Control Performance of Pneumatic Rubber Artificial Muscle Manipulator by Using Electro-rheological Fluid Damper," *in Proc., IEEE, Int., Conf., Syst Man Cybernet*, Vol. 4, pp. 788~793.

Raparelli, T., Zobel, P. B. and Durante, F., 2001, "The Design of a 2 DOF Robot for Functional Recovery Therapy Driven by Pneumatic Muscles," *Int., Workshop on robotics in ALPA – DRIA -DANUBE region*

Raparelli, T., Zobel, P. B. and Durante, F., 2003, "Development of a Robot Driven by Pneumatic Muscles," *Proc., RAAD, Workshop on robotics in ALPA – DRIA - DANUBE region*

Thanh, T. D. C. and Ahn, K. K., 2006a, "Nonlinear PID Control to Improve the Control Performance of 2 Axes Pneumatic Artificial Muscle Manipulator Using Neural Network," *Accepted for Publication in Int., Jour., Mechatronics*

Thanh, T. D. C. and Ahn, K. K., 2006b, "Intelligent Phase Plane Switching Control of Pneumatic Artificial Muscle Manipulators with Magneto-rheological Barke," *in Int., Jour., Mechatronics*, Vol. 16, pp. 85~95.

Zobel, P. B., Durante, F. and Raparelli, T., 1999, "The Experience of the University of L'Aquila on the Pneumatic Muscle Actuators for a 2 DOF Manipulator for Function Recovery Therapy," *Seminar on Biomechanics*, Warsaw, Poland.